We are IntechOpen,
the world's leading publisher of Open Access books
Built by scientists, for scientists

6,900
Open access books available

186,000
International authors and editors

200M
Downloads

Our authors are among the

154
Countries delivered to

TOP 1%
most cited scientists

12.2%
Contributors from top 500 universities

CLARIVATE ANALYTICS
BOOK CITATION INDEX
INDEXED

WEB OF SCIENCE™

Selection of our books indexed in the Book Citation Index
in Web of Science™ Core Collection (BKCI)

Interested in publishing with us?
Contact book.department@intechopen.com

Numbers displayed above are based on latest data collected.
For more information visit www.intechopen.com

Fetal Central Nervous System Abnormalities

Andreea Ceausescu, Andreea Docea, Marina Dinu,
Stefan Degeratu, Dominic Iliescu and Monica Cara

Additional information is available at the end of the chapter

Abstract

Central nervous system (CNS) is one of the most frequent sites for prenatal diagnosed congenital abnormalities (10 per 1000 live births, much higher than the heart—eight per 1000, kidneys—four per 1000, and other fetal systems). Due to the evolving pattern, ultrasound screening for fetal brain malformations is usually performed at 19–22 weeks' gestation, but severe congenital anomalies can be diagnosed much earlier. This chapter is a short review, structured in eight subchapters: the first one is dedicated to the normal ultrasound aspect of different CNS segments, and the following ones are to detect pathology in prenatal life. We used many ultrasound images and tried to correlate the prenatal findings with the ones obtained postpartum/postabortum for each case, by means of pathology/imaging techniques.

Keywords: cortex, spine, cerebellum, brain stem, malformations, development

1. Introduction

It has been said that the central nervous system (CNS) is the most complex among the fetal and adult systems. This is one of the most common sites of congenital malformation, both in fetuses with and without chromosomal abnormality. It is extremely difficult to diagnose structural abnormalities or mild ultrasound (US) abnormalities that have been linked to major functional problems. Just the opposite, major anatomic defects may not lead to significant malfunctioning of the system. It is extremely important to study the structure, in an attempt to understand the function of the normal and abnormal fetal central nervous system [1, 2]. The detection of CNS anomalies in fetal life is feasible using modern ultrasound equipment. Many

anomalies of the central nervous system develop early, and nowadays, we have the tools to detect some conditions at 11–13 weeks [3–8] or even earlier. The first-trimester detection of CNS anomalies is probably the most important advance in modern sonoembriology. Later in pregnancy, neurosonography is a powerful tool in diagnosing CNS pathology.

The following chapter is structured as follows:

1. Normal findings

2. Ventricular system (ventriculomegaly, aqueduct stenosis)

3. Neural tube defects (NTDs) (anencephaly, encephalocele, myelomeningocele)

4. Cortical formation abnormalities (schizencephaly, lissencephaly, heterotopia, microcephaly)

5. Midline abnormalities (holoprosencephaly, complete/partial agenesis of corpus callosum or abnormal corpus callosum, absent cavum septum)

6. Posterior fossa abnormalities (mega cisterna magna, Blake's pouch cyst, Dandy-Walker or variant cerebellar, vermian hypoplasia)

7. Vascular abnormalities (hemorrhage, hematoma, dural fistula, aneurysms)

8. Destructive lesions (hydranencephaly, tumors/mass lesions, cysts, periventricular leu-komalacia, infections, dysplasias, other lesions).

2. Normal findings

Some intracranial segments of CNS are seen on ultrasound *extremely early* in development, especially when using high-resolution probes and modern electronic tools. Although many features are indeed recognizable, the clinical utility of such studies is yet to be proven (**Figures 1–3**).

In the *late first trimester*, current guidelines recommend checking for present cranial bones, for normal midline falx, and for the presence of choroid plexus and filled ventricles [9]. The most recommended planes for assessing the head anatomy are the axial ones. In terms of spine assessment, the guidelines state that "longitudinal and axial views should be obtained to show normal vertebral alignment and integrity, and an attempt should be made to show intact overlying skin" [9] (**Figure 4**).

From the early *second trimester* onwards, the commendation is to obtain in standard assess-ment three standard axial planes (transventricular, transthalamic, and transcerebellar), and, if technically feasible, the fetal profile [10] (**Figures 5** and **6**).

The measurements for fetal head *biometry* (the biparietal diameter—BPD and the head circum-ference—HC) are possible when using the transventricular (biventricular) and the transthalamic plane. In the most commonly used technique, the calipers are placed from the outer edge to the
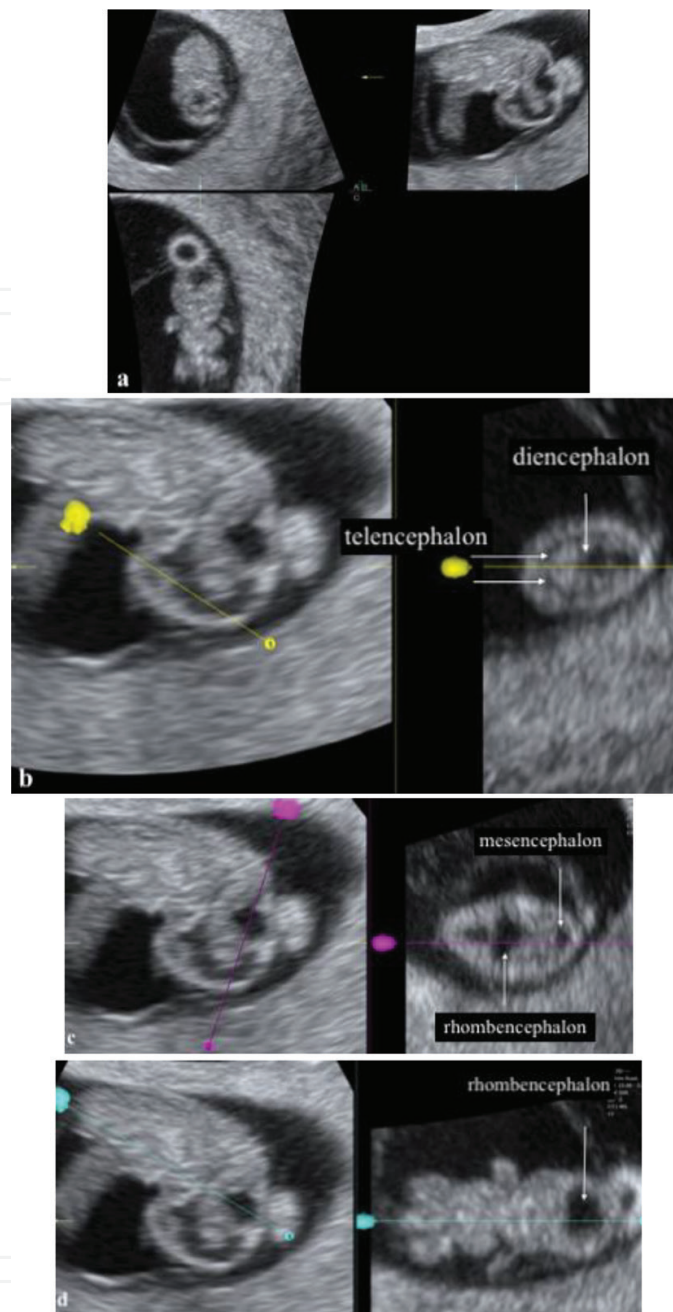
Figure 1. Dating ultrasound scan at 8 weeks of amenorrhea (WA) and 3 days (d). Volumetric ultrasound: sectional planes in the multiplanar mode (a). Subsequently, OmniView facility was used, the line mode (b, c, and d). The embryonic central nervous primitive vesicles can be observed.

inner edge (the "leading edge" technique), at the widest part of the skull, using a perpendicular angle to the midline falx. The HC is measured on the external contour. The cranial bones describe on axial planes a regular *ovoid* shape. The *midline* must be continuous, having no deviations, and the intracranial structures must be symmetrical, mirroring each other's half. Usually, the proximal hemisphere to the probe has a lower visibility, and only the distal one is described by the operator. On the *transthalamic plane*, the anatomic landmarks are (from anterior to posterior) the frontal horns of the lateral ventricles (LVs), the cavum septi pellucidi (CSP), located between
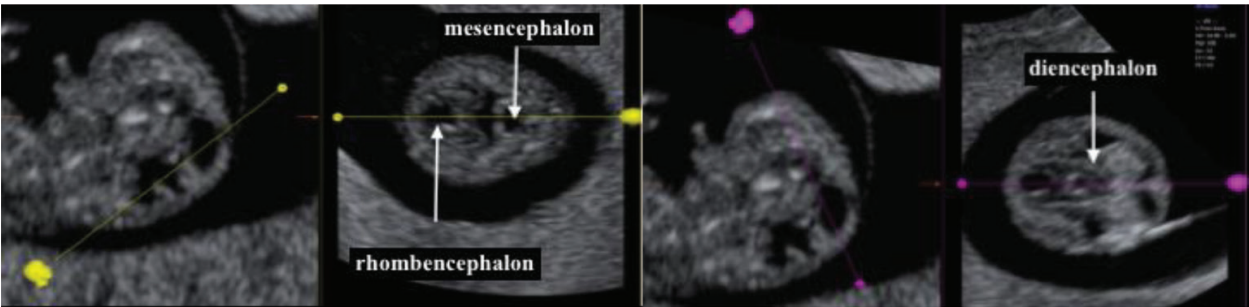
Figure 2. The same case, at 10 WA 1d. The same technique was used, after acquiring a static 3D volume.
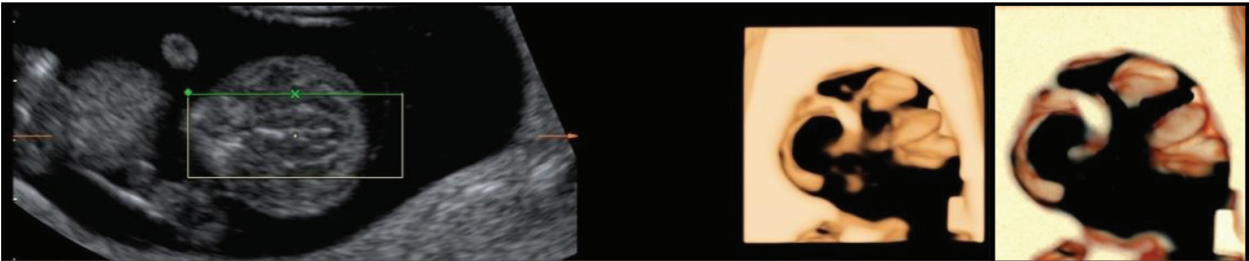

Figure 3. The same case, at 10 WA 1d. The region of interest is placed inside the head, and HD (high-definition) inversion mode surface rendering is applied. This imaging technique acts like a matrix, or a "mold," bringing forth fluid-filled cavities: the early ventricular system.
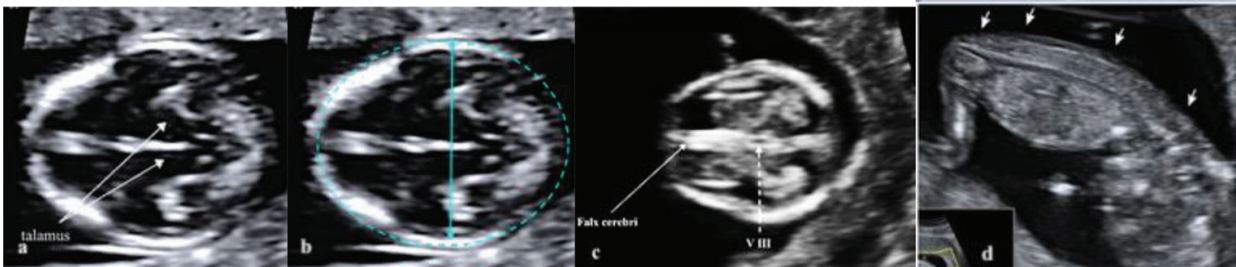

Figure 4. The thalamic plane (a and b), the third ventricle plane (c), and the longitudinal image of the spine, in a prone position (d). In b, the head biometry is represented (measurement of BPD and HC).

them as a fluid-filled structure, the two thalami (resembling together a "heart image"), the third ventricle between them, and the hippocampal gyrus. The *biventricular plane* is found just above the previous one and allows the visualization of the lateral ventricles, with the choroid plexus inside them. The width of the posterior horn of the lateral ventricle must be measured using the exact mark of the parieto-occipital sulcus, inside the echoes generated by the ventricular walls, by a direction aligned perpendicularly to the long axis of the ventricle. Before 25 WA, the measurement must be smaller than 8 mm. The *transcerebellar plane* is obtained just below the transthalamic one, in an oblique fashion. The slight posterior tilting allows the visualization of the frontal horns of the lateral ventricles, CSP, thalami, cerebellum, and cisterna magna [1, 10]. The transversal diameter of the cerebellum (in mm) equals roughly the gestational age (in weeks). In
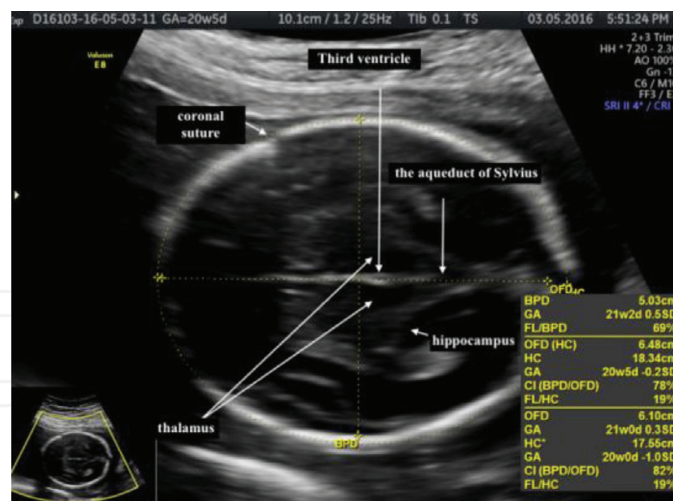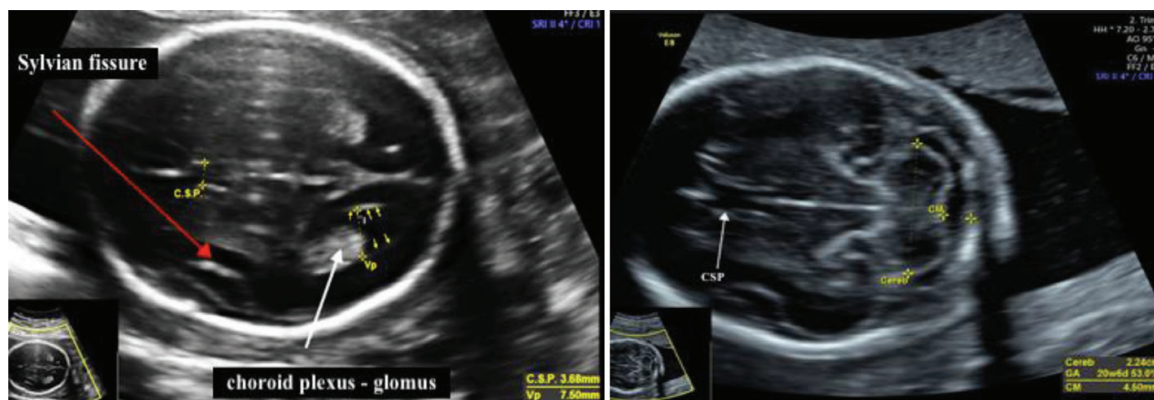
Figure 5. The thalamic plane.

Figure 6. The biventricular (transventricular) and the transcerebellar plane.

the second half of gestation, the depth of the cisterna magna (measured between the cerebellar vermis and the intern margin of the occipital bone) is stable and should not exceed 10 mm.

The *neurosonogram* implies obtaining four more coronal planes and three sagittal/parasagittal planes and assessing the evolving cerebral fissures, gyrations, and circumvolutions [1]. The coronal planes are displayed in **Figure 7**.

The *transfrontal* plane is obtained through the anterior fontanelle. The interhemispheric fissure (IEF) in the median plane and the anterior horns of the lateral ventricles on both sides can be seen. This plane passes anterior to the genu of the corpus callosum (CC), and this is why the IEF appears uninterrupted. The *transcaudate* plane passes at the level of caudate nuclei and the genu of the CC. It interrupts the continuity of the IEF. CSP appears as an anechogenic triangular structure under the CC. Lateral ventricles are seen, surrounded by the cortex. Also, the Sylvian fissures may be identified, laterally. In the *transthalamic* plane, the thalami are seen adjoining. In some cases, the third ventricle is seen in the median plane. In this plane, at the base of the skull, the vessels of the circle of Willis and the optic chiasma
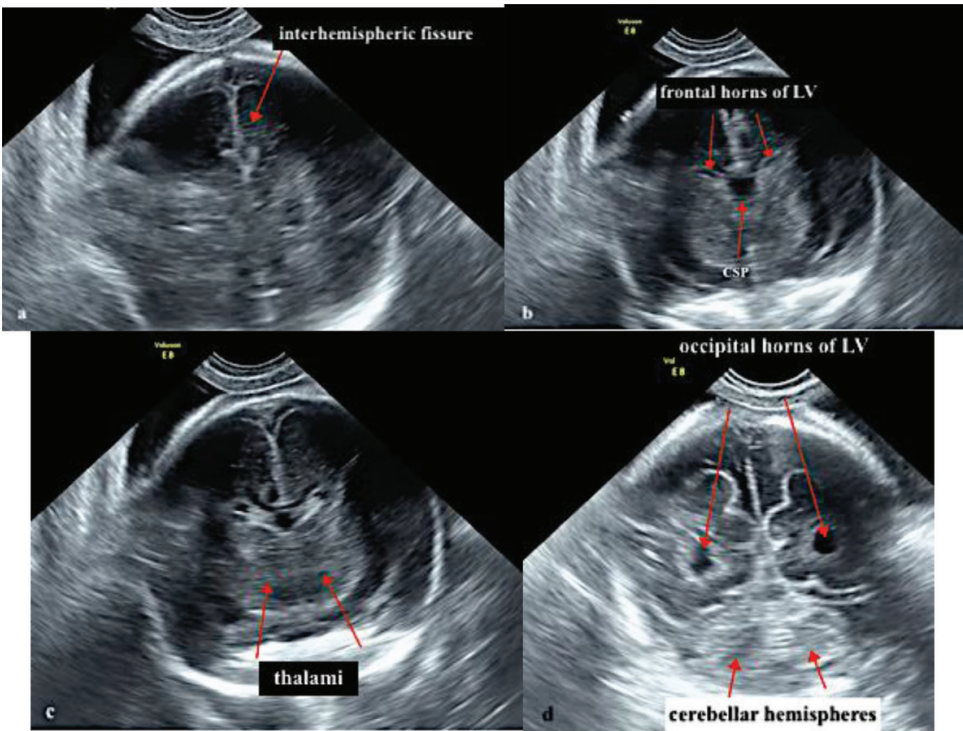
Figure 7. The transfrontal plane (the frontal-2), the transcaudate plane (mid-coronal-1), the transthalamic plane (mid-coronal-2), and the transcerebellar plane (occipital-1 and 2).

may be recognized. The *transcerebellar* plane is obtained through the posterior fontanelle. The occipital horns of the LV and IEF are seen, also the cerebellar hemispheres and the vermis.

The antero-posterior planes are displayed in **Figures 8** and **9**.

In the *midsagittal* (median) plane, all components of the CC (rostrum, genu, body, splenium) may be seen. Also, the CSP, the brain stem, pons, vermis, and posterior fossa. The parasagittal planes (right and left) depict the entire LV, the choroid plexus, the periventricular tissue, and the cortex.
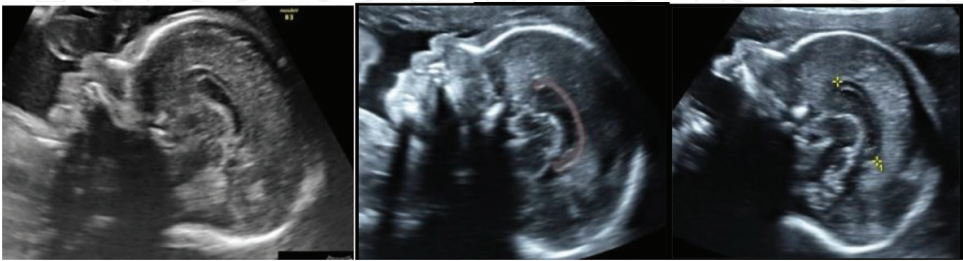

Figure 8. The sagittal plane. The corpus callosum is highlighted in the middle image.
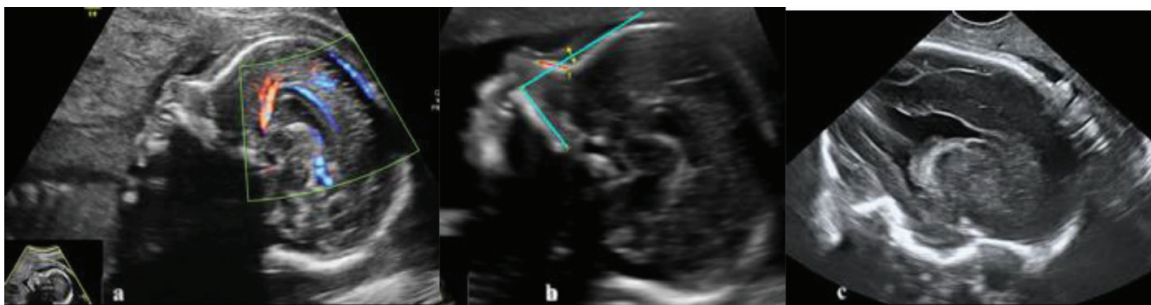
Figure 9. The sagittal plane with HD flow applied, displaying the pericallosal artery (a), the measurement of the nasal bone and the fronto-maxillary facial angle, and the parasagittal or oblique plane-1 (c).

2.1. The spine

In the sagittal and parasagittal planes, the ossification centers of the vertebral body and posterior arches form two parallel lines that converge in the sacrum, in the prone position of the fetus. Efforts must be made to demonstrate the integrity of the overlying skin.

In the second and third trimesters, these planes allow imaging of the spinal canal and of the spinal cord within it. The conus medullaris is usually found at the level of L2–L3 vertebrae (**Figure 10**).

In transverse planes or axial planes, the vertebrae have different shapes at different levels [1]. Fetal thoracic and lumbar vertebrae have a triangular shape, the first cervical vertebrae are quadrangular in shape, and sacral vertebrae are flat.

The normalcy of the vertebrae and ribs' arches may be very easily demonstrated in the coronal plane, using the 3D technique, skeletal mode. Both can be readily numbered (**Figure 11**).

In the prenatal scanning, many normal and abnormal structures may vary and evolve intensively. Thus, using descriptive terms is advisable. The observer may use a thorough detailed depiction of the visualized structures and features, may note the absent normal structure/ structures, and may signalize an abnormal structure. This approach is preferred to issuing a specific diagnosis.
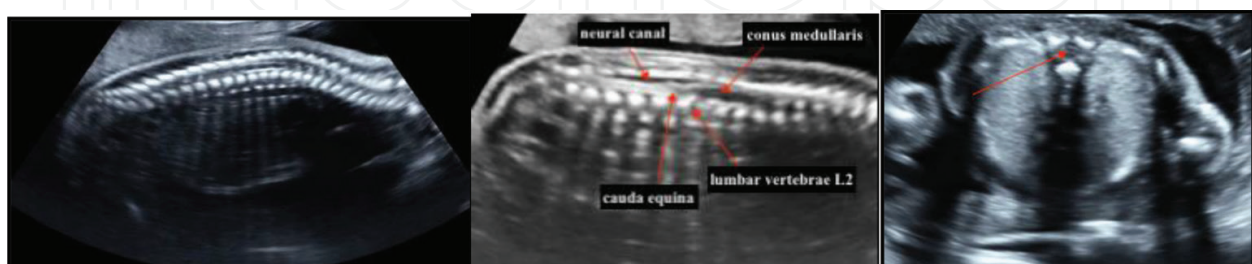

Figure 10. The imaging of the spine and the distal region of the spinal canal. Axial thoracic vertebrae.
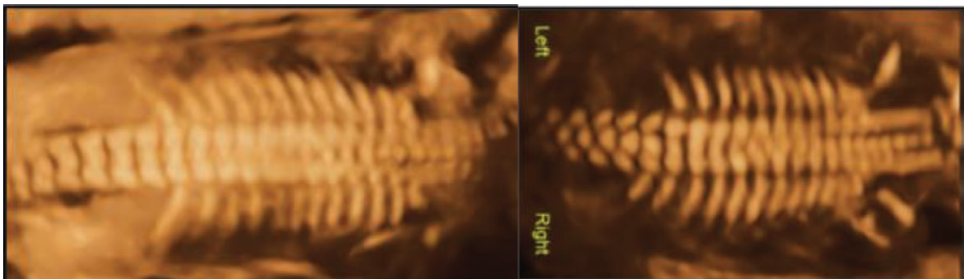
Figure 11. Imaging the spine in the coronal plane. In left image, a supernumerary lumbar rib case is shown.

3. Abnormalities of the ventricular system

Ventriculomegaly is the most frequent abnormal CNS finding diagnosed in utero and is the most common indication for second-level neurosonography and fetal magnetic resonance imaging (MRI) [11].
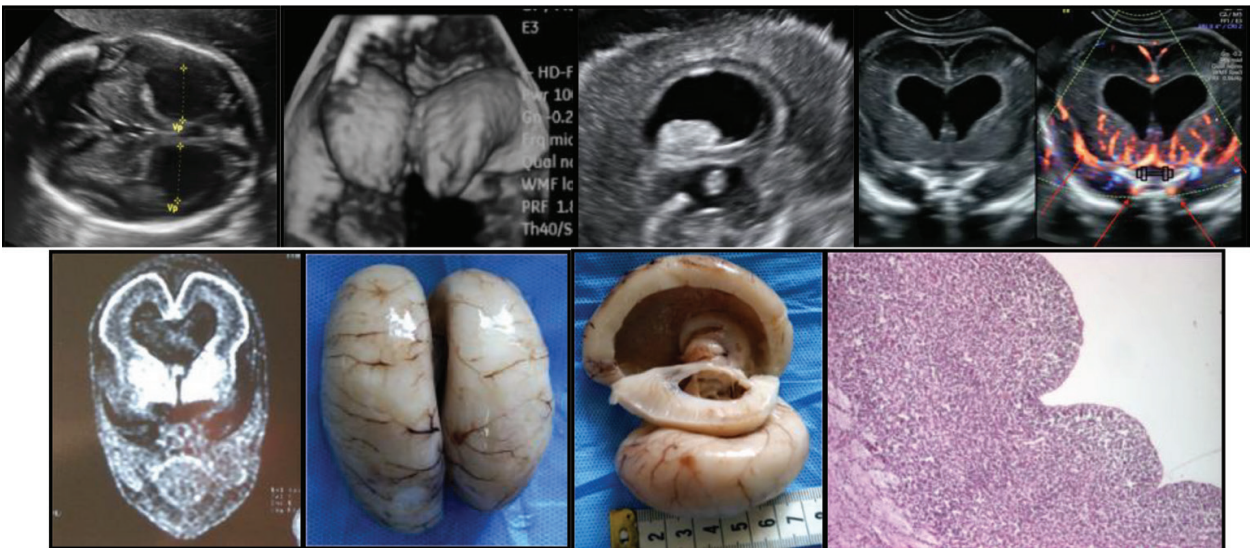

Figure 12. Early ventriculomegaly cases.

Figure 13. Severe obstructive ventriculomegaly, with unknown origin. Pathologic differentiation of diencephalon and mesencephalon. Conventional necropsy confirms the enlarged ventricles. Microscopy: marked astrocyte cell line proliferation, neuronal migration defects, and cortical fibrosis (stained with hematoxylin and eosin, ob. 40×).

Establishing its class of severity is based on the width of the atrium of the lateral ventricle measurement: ventriculomegaly is considered to be mild when the atrial width is 10–12 mm, moderate between12 and 15 mm, and severe if larger than 15 mm.

In rare cases, ventriculomegaly is accessible in early pregnancy (**Figure 12**).

Yet, this is usually a second- and third-trimester diagnosis. The prevalence of mild ventriculomegaly, based on current criteria, is estimated to be around 0.7% [12]. The finding of ventriculomegaly should trigger a thorough analysis of the fetal brain to investigate all associations (malformative, clastic, tumoral, and syndromic). If no underlying pathophysiology and etiology are found, ventriculomegaly is referred to as "isolated." Melchiorre et al. [13] demonstrated the particularly difficult counseling in such cases. Aqueductal stenosis is the most common cause of ventriculomegaly and its extreme form—fetal hydrocephalus. Published studies of neonates with aqueductal stenosis have noted variable outcomes, with normal development seen in 24–86% of cases [14] (**Figures 13–15**).
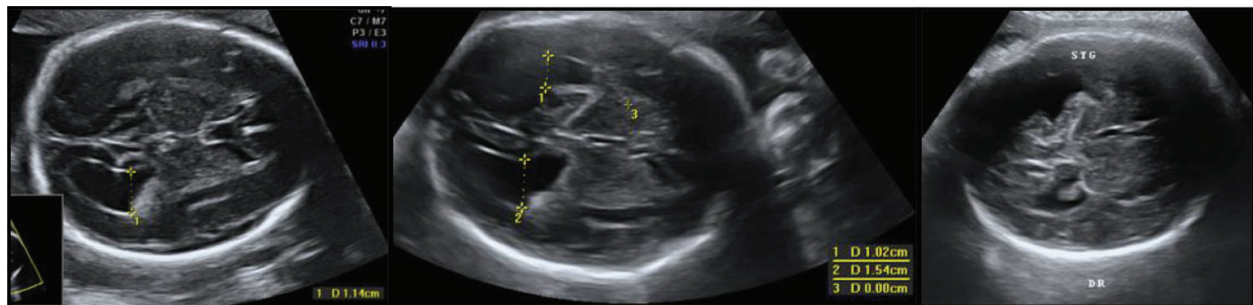
Figure 14. Different cases of unilateral borderline isolate ventriculomegaly, symmetric, and asymmetric.
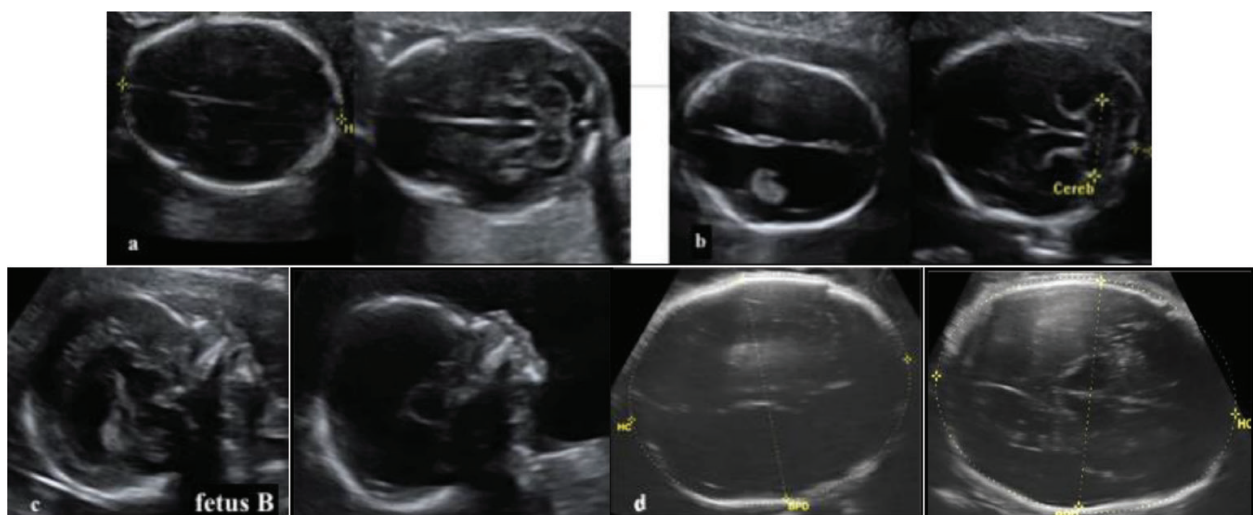
Figure 15. Twin monochorionic diamniotic pregnancy, with discordant major SNC anomaly: severe ventriculomegaly due to aqueductal stenosis. The images display comparatively the same planes: the transthalamic (a) and transcerebellar plane (b), the fetal profile (c) at 17 WA. The transthalamic plane at 25 WA (d). The long-term evolution of fetus B was favorable (after ventriculo-peritoneal shunt).

4. Neural tube defects

Neural tube defects (NTDs) are a frequent group of severe anomalies of the central nervous system. The most frequent conditions are anencephaly, spina bifida, and cephalocele [15]. The open NTDs occur as a result of a primary failure of the neural tube closure between the 17th and 30th postfertilization days. They have a rather stable prevalence. This highlights the importance of primary prevention by folic acid supplementation and the paramount meaning of accurate prenatal diagnosis. In rare cases, some forms of NTDs may be recognized very early in pregnancy (**Figure 16**).

Yet, the vast majority of cases are approached in the late first trimester (11–13 WA), due to the fact that the role of this scan has evolved [5, 7, 8, 16–18]. The technique has grown, no longer being a screening for aneuploidy tool [19–22]—but a method to almost assess the complete fetal anatomy. This became the first anomaly scan in many units [4, 5, 18, 23–25].

In terms of central nervous system, the newest area of debate is the significance of posterior fossa ultrasound semiology. At 11–14 weeks of gestation, it is possible to visualize and measure many spaces in the posterior brain: the brainstem (BS), the fourth ventricle or intracranial translucency (IT), and the cisterna magna (CM). In some settings, such anatomical spaces are assessed routinely by ultrasound in parasagittal or oblique views of the fetal face, as part of the nuchal translucency (NT) scan [26, 27]. Abnormalities of the posterior brain spaces or deviations of their measurements have been proposed as markers of congenital malformations of the posterior fossa [26–29]. Subsequently, the correlation between the decreased amount of intracranial fluid and open spina bifida (OSB) has been established [16, 30]. More recently, it has been suggested that increased fluid may indicate the presence of cystic posterior fossa anomalies such as Dandy-Walker malformation (DWM) and Blake's pouch cyst (BPC) [31–35].

Also, the axial planes offer many indirect signs of OSB and have competed with the sagittal planes in the efficacy of first-trimester screening for OSB [36–38]. It seems that in experienced hands, OSB may reach 100% early detection rates, being reliably diagnosed at 11–14 weeks of screening [39].

In our view, both sagittal and axial planes of the fetal head may be used in OSB screening, depending on the operator's skills and the equipment used. Also, the small BPD may be useful [40, 41].

Figure 16. Early embryonic demise, in a case of suspected exencephaly.

2D planes and markers for fetal central nervous system (CNS) morphologic assessment at the first-trimester ultrasound scan are shown in **Figure 17**: left column, a normal fetus; right column, isolated OSB fetus.

In the thalamic plane, the regularity of the skull and the bone ossification should be assessed. Also, measurements may be performed: the biparietal diameter (BPD), the head circumference (HC), and optional—the occipito-frontal diameter (OFD). Thalamus, the third ventricle (red arrow), and symmetry of the intracranial structures may be subjectively assessed. In this plane, the "crash sign" may be subjectively evaluated (the aqueduct of Sylvius position) or the distance between this feature and the occipital bone may be measured (the aqueduct—indicated by the blue quadrant, and mesencephalon—normal by the yellow contour and pathologic by the red contour).

In the lateral third-ventricle plane, aside from the regularity of the skull and the bone ossification assessment, the following structures should be visualized: the midline falx echo, the choroid plexuses, the interhemispheric fissure, the posterior horns of the lateral ventricles (LVs), the lateral walls of the anterior horns of the LV, and the thin brain mantle. In this plane, the "dry brain phenomenon" is usually present in OSB cases: the subjective large choroid plexus for the skull (**Figure 18**).

In the sagittal plane (often called the *mid-sagittal* plane), many CNS structures may be identified and measured: the thalamus (T), the brain stem (BS), the medulla oblongata (MO), the midbrain (M), and the future cisterna magna (CM). In OSB cases, some mild signs may be found: the alteration of the BS (brainstem diameter)/BSOS (brainstem to occipital bone diameter) ratio and the decreased frontomaxillary facial (FMF) angle. The most valuable in screening seems to be the alteration of the cisterna magna (**Figure 19**).

Along with the mild early signs of spinal neural tube defects, other major malformations reach 100% detection rates in many reports. **Figures 20–22** show several such cases, showing correlations between the ultrasound data and the specimen aspects.
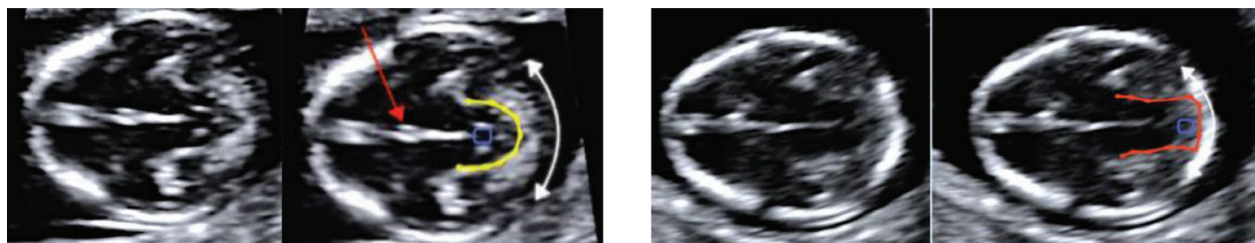

Figure 17. The transthalamic view of cranium in a normal (left) and an OSB case (right).
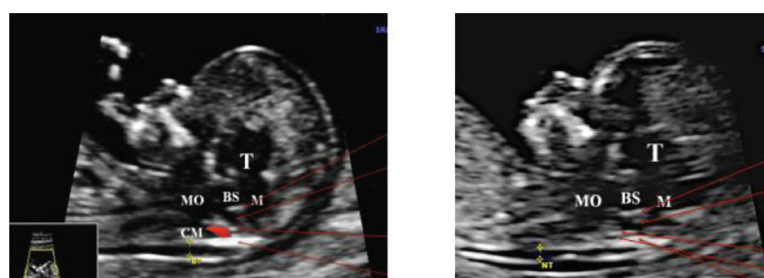

Figure 18. The sagittal plane of cranium in a normal (left) and an OSB case (right).

Figure 19. Rachischisis. Medical termination of pregnancy at 16 WA. 3D ultrasound in a surface-rendering mode (a), pathologic specimen (schisis of the lumbar skin, with exposing the meninges and the spinal canal structures) and MRI details of specimen, confirming the hemivertebra suspected on US.

Figure 20. Exencephaly. Ultrasound images and the pathologic specimen at 12 WA.

Figure 21. Encephalocele at 12 W. Conventional 2D ultrasound and 3D surface rendering.

Figure 22. Complex lethal facial and cerebral anomaly. The red arrow indicates the single orbit. The pathologic specimen confirms ciclopy, proboscis, exencephaly (a). Second-trimester case of anencephaly: 2D conventional and 3D ultrasound (b).

5. Cortical formation abnormalities

The cerebral *cortex development* implies evolvement through three steps: neuronal precursor proliferation and differentiation; migration of immature neurons; and cortical maturation (the laminar organization and occurrence of synapsis). Neurons migrate from the ventricular zone (called the germinal matrix) toward the pial surface, along radially oriented glial scaffolds [42–44]. Gyration and sulcation occur afterword, beyond 32 WA. Disruption of any of these steps in cerebral development, due to inherited or acquired causes, can result in a wide spectrum of abnormalities.

Schizencephaly is a congenital cerebral defect in clefting, where clefts extend through the hemispheres from the ventricles to the pial surface [45]. Having two clinical types (open and closed), it seems to be caused by a primary failure of development of the cerebral mantle in early pregnancy. The condition is different from *porencephaly*, being characterized by the presence of heterotopic gray matter lining the cleft. Although primary, it has also been reported as a destructive process mediated by vascular injury also.

Lissencephaly means literally "smooth brain." This is a rare brain malformation, gene-linked, characterized by the absence of normal convolutions in the cerebral cortex, leading to *microcephaly*. In most cases, neonates have usually a normal sized head at birth. The "cobblestone lissencephaly" is characterized by the irregular surface of the brain on the pathological specimen. This is due to aberrant neuroglial overmigration into the subarachnoid space. The formation of an extracortical agyric neuroglial layer occurs. It seems that the primary cause is the deficit of glycosylation of dystroglycans, resulting in neuroglial overmigration [44–50].

The presence of neurons in any position other than the cortex is called *neuronal heterotopia*. This is caused by an abnormal phenomenon of migration during fetal development. The most frequent type is *periventricular* heterotopia, given by an abnormal development of the neuroependyma [44, 50]. It consists of groups of disorganized neurons and glial cells that are located along the walls of the lateral ventricles. They may be isolated (X-linked and non-X-linked forms) or associated with other CNS malformations. The prevalence in the general population is unknown, but it has been related with epilepsy, seizures, and/or developmental delay, with different grades of severity. The prenatal diagnosis has been reported, but the condition is underdiagnosed in the vast majority of screening settings. The true *microcephaly* is considered part of a complex disorder [48–51], occurring in syndromes (with or without chromosomal anomalies). It may be associated exclusively with cerebral anomalies (due to either primary cerebral maldevelopment or clastic events like the ischemohemorrhagic ones) or infectious diseases; the latter has gained a particular interest lately, in light of the recent emergence of microcephaly related to Zika virus infection [48–51]. *Macrocephaly* may result from macrocrania, hydrocephalus, or a major subarachnoid space abnormality. If not associated with other conditions, macrocephaly is synonymous with megalencephaly, meaning an increase in the weight and size of the brain [52] (**Figure 23**).
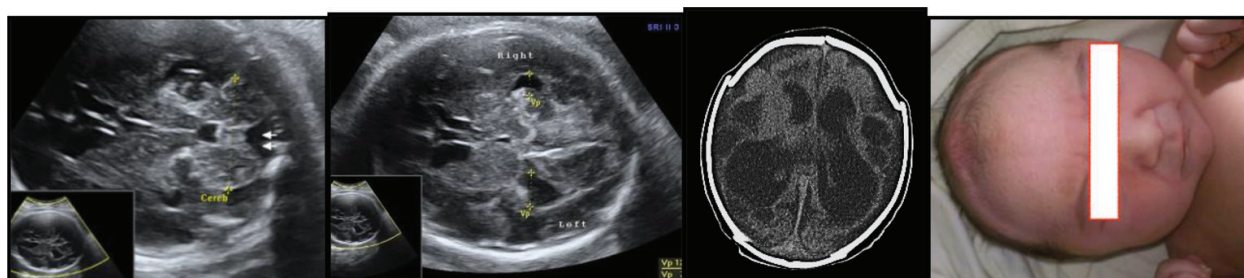
Figure 23. Complex cortical anomaly. Nodular periventricular heterotopia seen. Cortical hypoplasia. Microcephaly. Periventricular leukomalacia. The postpartum image highlights the abnormal excessive ossification of the coronal suture and the dysmorphic facial features of the neonate.

6. Midline abnormalities

Holoprosencephaly is a congenital induction disorder, occurring extremely early in pregnancy (3–6 WA), with failing the segmentation of the neural tube [53–57]. This leads to incomplete separation of the prosencephalon. It has been classified into four subtypes: alobar, semilobar, lobar, and a middle interhemispheric fusion variant (syntelencephaly).

The alobar holoprosencephaly is the most severe type, having a complete lack of separation of the cerebral hemispheres; this lead to a single ventricle, absence of the CC and IEF, and fused thalami. In the semilobar type, the cerebral hemispheres are fused anteriorly. In lobar holoprosencephaly, the fusion of the cerebral hemispheres is present at the frontal lobes. The middle interhemispheric fusion variant results from nonseparation of posterior frontal and parietal lobes.

The *corpus callosum* is the largest commissure of the brain, and its development is accelerated between 8 and 20 WA. Any disturbance of this process may lead to CC agenesis or partial agenesis (hypogenesis or dysgenesis). Many CC abnormalities (in terms of dimensions and shape) are frequently diagnosed during pregnancy although their significance is still debated [58–67]. Abnormal CC has been described among patients assessed for mental retardation.

In a similar way, the absence of fluid in the CSP (with or without intact *septum pellucidum* and corpus callosum) may indicate subtle or severe midline brain abnormalities. All these conditions may have significant implications for postnatal neurological development [58, 61, 63–68] (**Figures 24** and **25**).
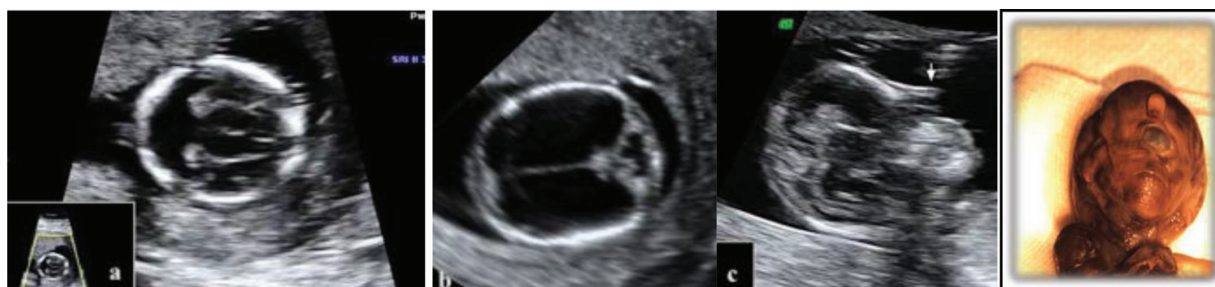

Figure 24. Different cases of holoprosencephaly in the first trimester (a,b). c. a case which associates proboscis.

Figure 25. Second-trimester alobar holoprosencephaly (a and b). Short and thick corpus callosum (c).

7. Posterior fossa abnormalities

Posterior fossa abnormalities include the Dandy-Walker malformation (complete or partial agenesis of the cerebellar vermis, cystic dilatation of the fourth ventricle, and enlarged posterior fossa, with upward displacement of the tentorium, torcula, and transverse sinuses); the mega cisterna magna (a CM measuring more than 10 mm and a normal vermis); the Blake's pouch cyst (the presence of an upwardly displaced normal cerebellar vermis, normal appearance of the fastigium, tentorium, and size of the cisterna magna); and isolated vermian hypoplasia (a normally formed vermis but of smaller size, with an otherwise normal size and anatomy of the posterior fossa) [69, 70]. It seems that the Dandy-Walker malformation, even if apparently isolated on ultrasound imaging, carries a high risk for chromosomal and associated structural anomalies. Isolated mega CM and Blake's pouch cyst have a low risk for aneuploidy and associated structural anomalies. The isolated vermian hypoplasia is extremely rare; thus, the literature does not offer definite conclusions about its significance. This needs to be further assessed (**Figure 26**).
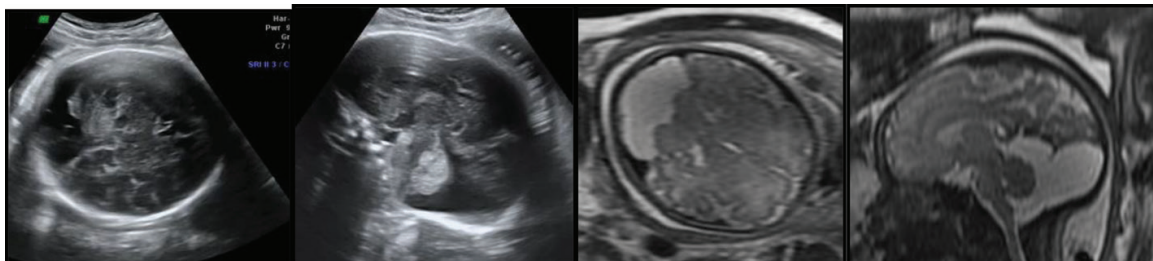
Figure 26. Isolated mega cisterna magna. US and MRI images of the same third-trimester case.

8. Vascular abnormalities

Possible causes of hemorrhage include arteriovenous malformation, benign or malignant, intracranial tumors, fetal infection, drug toxicity, and clotting disorders, such as isoimmune or alloimmune thrombocytopenia [71–79].

Fetal *hemorrhagic* and *hypoxic-ischemic* insults can lead to antenatal brain damage and fetal stroke. These are associated with fetal death, postnatal seizures, mental retardation, psychomotor delays, and cerebral palsy [72]. Fetal intracranial hemorrhages and strokes can be

prenatally diagnosed by ultrasound and MRI. The classification of intracranial hemorrhages includes five major types: intraventricular hemorrhage, cerebellar, subdural, primary subarachnoid hemorrhages, and other intraparenchymal hemorrhages. Intraventricular hemorrhage is the most common variety of neonatal intracranial hemorrhages and is characteristic of the immature brain. Intraventricular hemorrhages are subdivided according to their severity into four grades: the first three grades are limited to the ventricles, while the fourth grade includes parenchymal involvement.

The outcome of bleeding into the ventricles ranges from hemorrhage absorption and resolution without residual deficit, to brain damage, with neurological and mental deficits, epilepsy and in extreme cases to fetal or neonatal death. Different scoring systems have been developed to predict the prognostic significance of fetal intraventricular hemorrhage. They depend upon ventricular enlargement and the presence or absence of brain parenchymal damage [72–79].

Spontaneous antenatal subdural hemorrhage is rare [71].

Vein of Galen aneurysmal malformation is a rare congenital malformation (1% of all abnormalities of the fetal cerebral arteriovenous system [80]. It occurs in isolation, although there have been reported cases related to cardiac abnormalities or cystic hygroma. The current hypothesis is the early occurrence (between the 6 and 11 WA), as a result of the persistence of an abnormal connection between the primitive choroidal vessels and the proximal region of the prosencephalic median vein. The persistence of the connection leads to the appearance of some abnormal arteriovenous shunts and the formation of the vein of Galen (**Figures 27** and **28**).
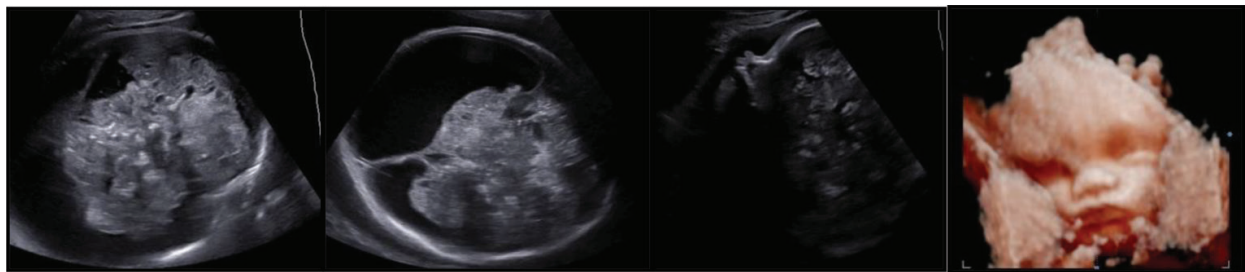

Figure 27. Massive intraparenchymatous hemorrhage in a case of fetal/neonatal alloimmune thrombocytopenia.

Figure 28. The same case. The fetus has had a complete normal neurosonogram in mid-trimester.

9. Destructive cerebral lesions

The destructive lesions may include an extremely wide range of conditions: hydranencephaly, tumors/mass lesions, cysts, periventricular leukomalacia, infections, dysplasias, intracranial hemorrhage, and other lesions. Identification of these abnormalities can be extremely helpful in providing the patients with management options. Moreover, it has the potential to modulate the neonatal therapy [81–85].

Hydranencephaly is a severe congenital condition: most of the cerebral hemispheres are replaced by a membranous sac. The pathogenic mechanism and the prognosis remain controversial. Still, fetal and postnatal neuroimaging data and histopathologic findings suggest an early bilateral internal carotid artery occlusion occurring at 8–12 WA [81].

Fetal brain *tumors* are rare and have a different histologic pattern [84]. The definitive diagnosis relies on histopathology. The distinction between potentially curable tumors and tumors rapidly fatal after birth is extremely difficult. Moreover, some intracranial masses are not real tumors. Among the histological structure, we mention teratoma, glioblastoma, fetus-in-fetu, craniopharyngioma, and hemangioma.

The acronym TORCH is used to refer to congenital *infections*: toxoplasmosis, other infections (syphilis, varicella zoster, and parvovirus B19), cytomegalovirus, and herpes simplex virus. Zika virus has emerged as an important worldwide congenital infection. Many maternal and fetal symptoms are common. All mentioned infections may cause neurologic damage (ventriculomegaly, intraventricular adhesions, subependymal cysts, intracerebral calcifications, and microcephaly). The Zika virus leads to a more severe spectrum of CNS abnormalities and affects mildly other organ systems [85]. All congenital infections have rather nonspecific ultrasound findings. For the imagist professional, the awareness of imaging features of common congenital infections may facilitate early diagnosis and may, at times, lead to prompt initiation of therapy.

Periventricular leukomalacia has been reported in preterm and growth-restricted fetuses and neonates, and in monochorionic complicated pregnancies. It manifests as punctate white matter lesions or focal white matter necrosis. In clinical settings, cranial US has a limited sensitivity in detecting them. MRI is a more useful tool [78, 86].

Unfortunately, *cortical dysplasias*, involved as an epileptogenic substrate, are the most subtle lesions to identify, diagnose, and characterize [87, 88]. Improved MRI techniques with a multimodality approach (magnetoencephalography, positron emission tomography) will probably increase sensitivity and specificity for identifying them.

The most used classification [88] tried to unify the terminology of cortical dysplasias, which are seen as a subset of all malformations of cortical development. This proposal is based on histopathologic data, clinical and imaging findings, being currently under review [87] (**Figures 29–31**).
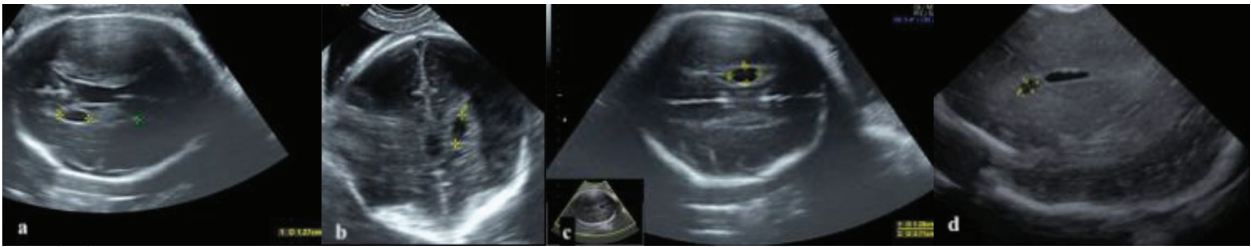
Figure 29. Benign, small dimensions, non-evolving intracerebral cyst: 28 WA (a and b), 30 WA (c), and postpartum, by means of transfontanellar ultrasound assessment (d).
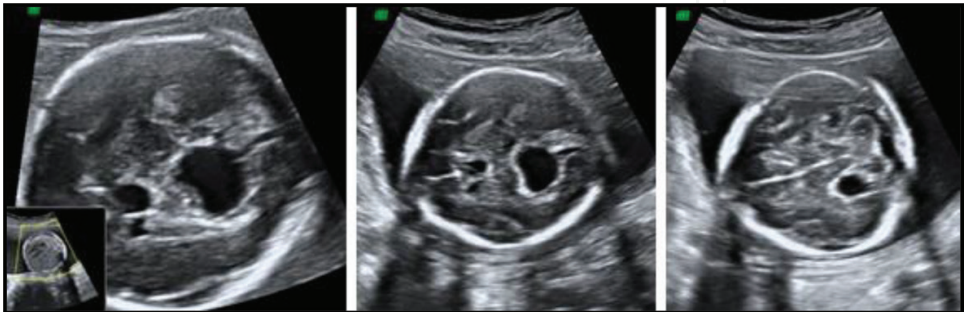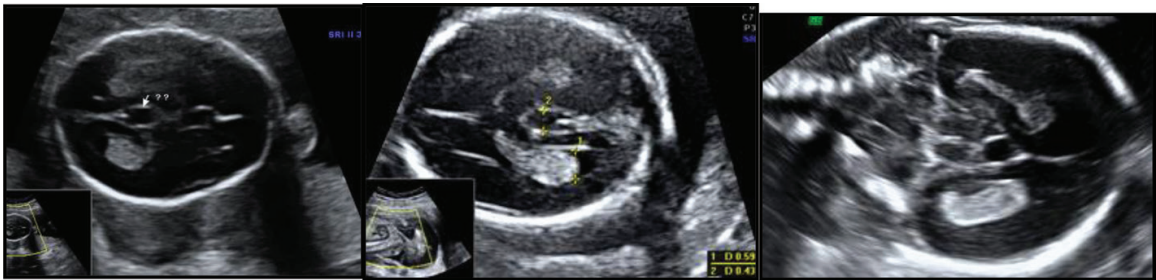

Figure 30. Porencephaly.

Figure 31. Arachnoid cyst.
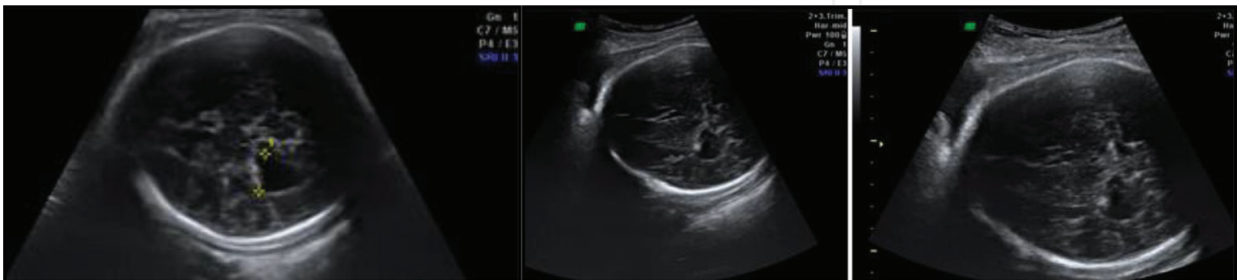
Figure 32. Midline abnormality and unilateral asymmetric borderline ventriculomegaly.

The above division of CNS congenital anomalies is an arbitrary one. In the most severe cases, several types of cortical malformation may be found simultaneously. Moreover, many types succed one another, or overlap in time.

Figures 32–34 show several examples of such associated abnormalities.
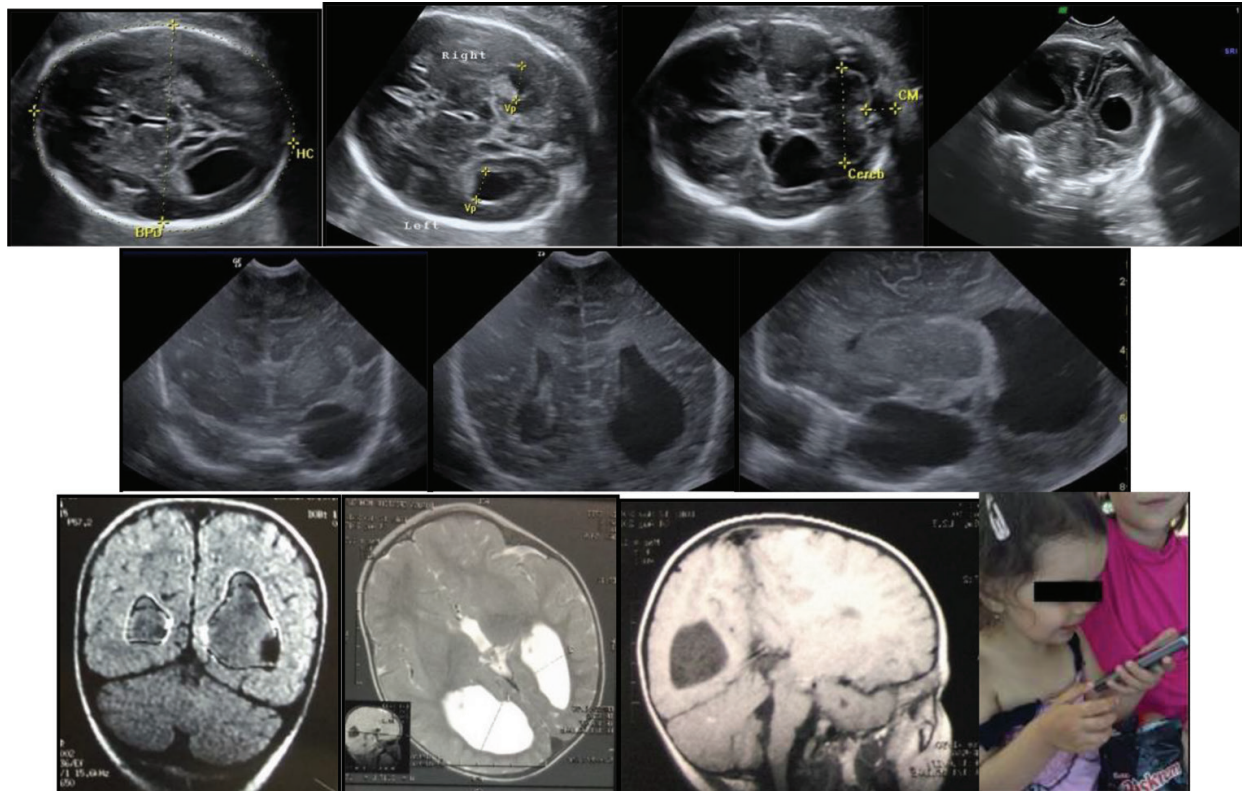
Figure 33. Complete agenesis of the corpus callosum. Unilateral voluminous intracerebral cyst. Severe unilateral asymmetric ventriculomegaly. Subsequently, the short-term and long-term evolution was completely normal.
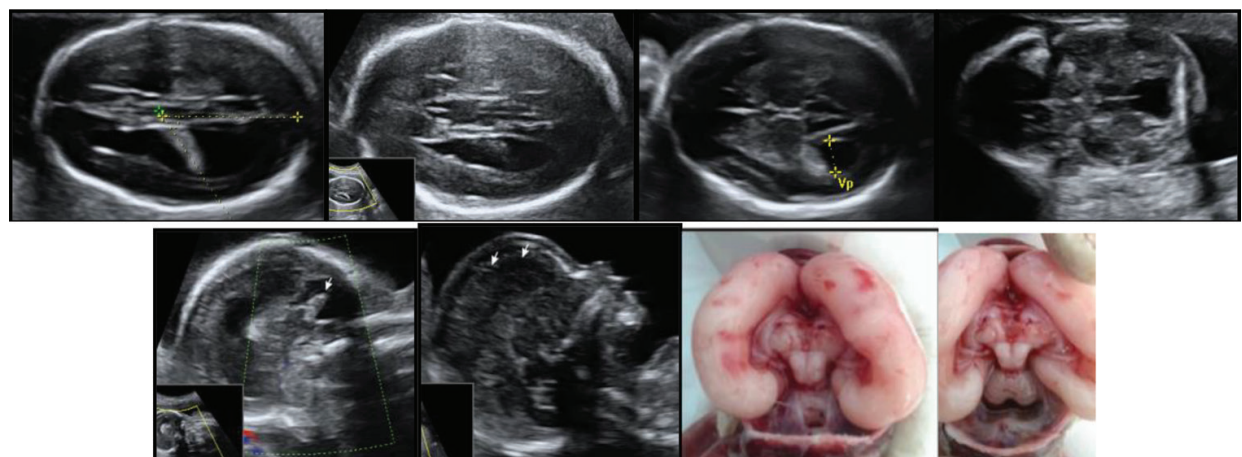
Figure 34. Complete agenesis of the corpus callosum. Cystic dilatation of the fourth ventricle and enlarged posterior fossa, with upward displacement of the tentorium, torcula, and transverse sinuses. Confirmation of the absence of CC by means of conventional autopsy.

Author details

Andreea Ceausescu[1]*, Andreea Docea[1], Marina Dinu[1], Stefan Degeratu[2], Dominic Iliescu[3] and Monica Cara[4]

*Address all correspondence to: and_deea2006@yahoo.com

1 Department of Obstetrics and Gynecology, Emergency University Hospital, Craiova, Romania

2 Department of Obstetrics and Gynecology, University Hospital, Craiova, Romania

3 Prenatal Diagnostic Unit, University of Medicine and Pharmacy of Craiova, Craiova, Romania

4 Department of Public Health, University of Medicine and Pharmacy, Craiova, Romania

References

[1] Sonographic examination of the fetal central nervous system: Guidelines for performing the 'basic examination' and the 'fetal neurosonogram'. International Society of Ultrasound in Obstetrics & Gynecology Education Committee. 2007;**29**:109-116

[2] Kurjak A, Antsaklis P, Stanojevic M, Vladareanu R, Vladareanu S, Neto RM, Barisic LS, Porovic S, Delic T. Multicentric studies of the fetal neurobehavior by KANET test. Journal of Perinatal Medicine. 2017;**45**(6):717-727

[3] Iliescu D, Comănescu A, Antsaklis P, Tudorache S, Ghiluşi M, Comănescu V, Paulescu D, Ceauşu I, Antsaklis A, Novac L, Cernea N. Neuroimaging parameters in early open spina bifida detection. Further benefit in first trimester screening? Romanian Journal of Morphology and Embryology. 2011;**52**(3):809-817

[4] Syngelaki A, Chelemen T, Dagklis T, Allan L, Nicolaides KH. Challenges in the diagnosis of fetal non-chromosomal abnormalities at 11-13 weeks. Prenatal Diagnosis. 2011;**31**:90-102

[5] Iliescu D, Tudorache S, Comanescu A, Antsaklis P, Cotarcea S, Novac L, Cernea N, Antsaklis A. Improved detection rate of structural abnormalities in the first trimester using an extended examination protocol. Ultrasound in Obstetrics & Gynecology. 2013;**42**(3):300-309

[6] Şorop-Florea M, Ciurea RN, Ioana M, Stepan AE, Stoica GA, Tănase F, Comănescu MC, Novac MB, Drăgan I, Pătru CL, Drăguşin RC, Zorilă GL, Cărbunaru OM, Oprescu ND, Ceauşu I, Vlădăreanu S, Tudorache Ş, Iliescu DG. The importance of perinatal autopsy. Review of the literature and series of cases. Romanian Journal of Morphology and Embryology. 2017;**58**(2):323-337

[7] Nemescu D, Dumitrescu A, Navolan D, Onofriescu M. First trimester three-dimensional ultrasound diagnosis of iniencephaly. A case report with review of literature. Gineco.eu. 2015;**11**:114-118. DOI: 10.18643/gieu.2015.114

[8] Dragusin R, Florea M, Iliescu D, Cotarcea S, Tudorache S, Novac L, Cernea N. The contribution and the importance of modern ultrasound techniques in the diagnosis of major structural abnormalities in the first trimester—Case reports. Current Health Sciences Journal. 2012;**38**(1):20-24

[9] Salomon LJ, Alfirevic Z, Bilardo CM, Chalouhi GE, Ghi T, Kagan KO, Lau TK, Papageorghiou AT, Raine-Fenning NJ, Stirnemann J, Suresh S, Tabor A, Timor-Tritsch IE, Toi A, Yeo G, International Society of Ultrasound in Obstetrics. ISUOG practice guidelines: Performance of first-trimester fetal ultrasound scan. Ultrasound in Obstetrics & Gynecology. 2013;**41**(1):102-113

[10] Salomon LJ, Alfirevic Z, Berghella V, Bilardo C, Hernandez-Andrade E, Johnsen SL, Kalache K, Leung K-Y, Malinger G, Munoz H, Prefumo F, Toi A, Lee W, on behalf of the ISUOG Clinical Standards Committee. Practice guidelines for performance of the routine mid-trimester fetal ultrasound scan. Ultrasound in Obstetrics & Gynecology. 2011;**37**:116-126

[11] Guibaud L, Lacalm A. Etiological diagnostic tools to elucidate 'isolated' ventriculomegaly. Ultrasound in Obstetrics & Gynecology. 2015;**46**(1):1-11

[12] Vergani P, Locatelli A, Strobelt N, Cavallone M, Ceruti P, Paterlini G, Ghidini A. Clinical outcome of mild fetal ventriculomegaly. American Journal of Obstetrics and Gynecology. 1998;**178**:218-222

[13] Melchiorre K, Bhide A, Gika AD, Pilu G, Papageorghiou AT. Counseling in isolated mild fetal ventriculomegaly. Ultrasound in Obstetrics & Gynecology. 2009;**34**:212-224

[14] Levitsky DB, Mack LA, Nyberg DA, Shurtleff DB, Shields LA, Nghiem HV, Cyr DR. Fetal aqueductal stenosis diagnosed sonographically: How grave is the prognosis? AJR. American Journal of Roentgenology. 1995;**164**(3):725-730

[15] Timbolschi D, Schaefer E, Monga B, Fattori D, Dott B, Favre R, Kohler M, Nisand I, Viville B, Astruc D, Kehrli P, Gasser B, Lindner V, Marcellin L, Flori E, Girard-Lemaire F, Dollfus H, Doray B. Neural tube defects: The experience of the registry of congenital malformations of Alsace, France, 1995-2009. Fetal Diagnosis and Therapy. 2015;**37**(1):6-17

[16] Garcia-Posada R, Eixarch E, Sanz M, Puerto B, Figueras F, Borrell A. Cisterna magna width at 11-13 weeks in the detection of posterior fossa anomalies. Ultrasound in Obstetrics & Gynecology. 2013;**41**(5):515-520

[17] Vladareanu R. Update in obstetrics and gynecology. Maedica (Buchar). 2011;**6**(1):66-67

[18] Tudorache S, Iliescu DG, Turcu A, Florea M, Dragusin R, Novac L, Cernea N, Cernea D. First trimester anomaly scan—The last redoubt won: Open Spina bifida. Donald School Journal of Ultrasound in Obstetrics and Gynecology. 2015;**9**(1):80-90

[19] Nicolaides KH. Screening for fetal aneuploidies at 11 to 13 weeks. Prenatal Diagnosis. 2011;**31**:7-15

[20] Burada F, Sosoi S, Iliescu D, Ioana M, Cernea D, Tudorache S. A rare occurrence of three consecutive autosomal trisomic pregnancies in a couple without offspring. Clinical and Experimental Obstetrics & Gynecology. 2016;**43**(2):287-290

[21] Sosoi S, Streata I, Tudorache S, Burada F, Siminel M, Cernea N, Ioana M, Iliescu DG, Mixich F. Prenatal and postnatal findings in a 10.6 Mb interstitial deletion at 10p11.22-p12.31. Journal of Human Genetics. 2015;**60**(4):183-185

[22] Calin FD, Ciobanu AM, Dimitriu MCT, Pacu I, Banacu M, Popescu I, Tarcomnicu IM, Ceauşu Z, Socea B, Paunica-Paunea G, Furau CG, Furau GO, Bacalbaşa N, Gheorghiu D, Ionescu CA. Edwards' syndrome diagnosis-between first trimester screening and ultrasound minor markers. Archives of the Balkan Medical Union. 2016;**51**(3):445-450

[23] Volpe P, Ubaldo P, Volpe N, Campobasso G, De Robertis V, Tempesta A, Volpe G, Rembouskos G. Fetal cardiac evaluation at 11-14 weeks by experienced obstetricians in a low-risk population. Prenatal Diagnosis. 2011;**31**:1054-1061

[24] Tudorache S, Cara M, Iliescu DG, Novac L, Cernea N. First trimester two- and four-dimensional cardiac scan—intra and interobserver agreement. Ultrasound in Obstetrics & Gynecology. 2013;**42**(6):659-668

[25] Becker R, Wegner RD. Detailed screening for fetal anomalies and cardiac defects at the 11-13-week scan. Ultrasound in Obstetrics & Gynecology. 2006;**27**:613-618

[26] Chaoui R, Benoit B, Heling KS, Kagan KO, Pietzsch V, Sarut Lopez A, Tekesin I, Karl K. Prospective detection of open spina bifida at 11-13 weeks by assessing intracranial translucency and posterior brain. Ultrasound in Obstetrics & Gynecology. 2011;**38**:722-726

[27] Egle D, Strobl I, Weiskopf-Schwendinger V, Grubinger E, Kraxner F, Mutz-Dehbalaie IS, Strasak A, Scheier M. Appearance of the fetal posterior fossa at 11+3 to 13+6 gestational weeks on transabdominal ultrasound examination. Ultrasound in Obstetrics & Gynecology. 2011;**38**:620-624

[28] Lachmann R, Picciarelli G, Moratalla J, Greene N, Nicolaides KH. Frontomaxillary facial angle in fetuses with spina bifida at 11-13 weeks' gestation. Ultrasound in Obstetrics & Gynecology. 2010;**36**:268-271. DOI: 10.1002/uog.7718

[29] Loureiro T, Ushakov F, Montenegro N, Gielchinsky Y, Nicolaides KH. Cerebral ventricular system in fetuses with open spina bifida at 11-13 weeks' gestation. Ultrasound in Obstetrics & Gynecology. 2012;**39**:620-624. DOI: 10.1002/uog.11079

[30] Volpe P, Contro E, Fanelli T, Muto B, Pilu G, Gentile M. Appearance of fetal posterior fossa at 11-14 weeks in fetuses with Dandy-Walker malformation or chromosomal anomalies. Ultrasound in Obstetrics & Gynecology. 2016;**47**(6):720-725

[31] Lachmann R, Sinkovskaya E, Abuhamad A. Posterior brain in fetuses with Dandy-Walker malformation with complete agenesis of the cerebellar vermis at 11-13 weeks: A pilot study. Prenatal Diagnosis. 2012;**32**:765-769

[32] Lee MY, Won HS, Hyunetal MK. One case of increased intracranial translucency during the first trimester associated with the Dandy-Walker variant. Prenatal Diagnosis. 2012;**32**:602-603

[33] Lafouge A, Gorincour G, Desbriere R, Quarello E. Prenatal diagnosis of Blake's pouch cyst following first-trimester observation of enlarged intracranial translucency. Ultrasound in Obstetrics & Gynecology. 2012;**40**:479-480

[34] Gandolfi Colleoni G, Contro E, Carletti A, Ghi T, Campobasso G, Rembouskos G, Volpe G, Pilu G, Volpe P. Prenatal diagnosis and outcome of fetal posterior fossa fluid collections. Ultrasound in Obstetrics & Gynecology. 2012;**39**:625-631

[35] Volpe P, Contro E, De Musso F, Ghi T, Farina A, Tempesta A, Volpe G, Rizzo N, Pilu G. Brainstem-vermis and brainstem-tentorium angles allow accurate categorization of fetal upward rotation of cerebellar vermis. Ultrasound in Obstetrics & Gynecology. 2012;**39**:632-635

[36] Tudorache S, Stiolica Turcu A, Iliescu DG, Florea M, Dragusin R, Cernea D. Modelling isolated spina bifida screening performance using axial and sagittal views of the brain and spine anatomy at the 11-13 week scan. Ultrasound in Obstetrics & Gynecology. 2015;**46**(S1):67

[37] Mangione R, Dhombres F, Lelong N, Amat S, Atoub F, Friszer S, Khoshnood B, Jouannic J-M. Screening for fetal spina bifida at the 11-13-week scan using three anatomical features of the posterior brain. Ultrasound in Obstetrics & Gynecology. 2013;**42**:416-420. DOI: 10.1002/uog.12463

[38] Ushakov F, Fernandez M, Lesmes Heredia C, Pandya P. OP06.08: "Crash sign": Displacement and deformation of mesencephalon against occipital bone in the diagnosis of spina bifida at 11-13 weeks. Ultrasound in Obstetrics & Gynecology. 2014;**44**:80. DOI: 10.1002/uog.13693

[39] Chen FC, Gerhardt J, Entezami M, Chaoui R, Henrich W. Detection of Spina bifida by first trimester screening—Results of the prospective multicenter berlin IT-study. Ultraschall in der Medizin. 2017;**38**(2):151-157

[40] Karl K, Benoit B, Entezami M, Heling KS, Chaoui R. Small biparietal diameter in fetuses with spina bifida on 11-13-week and mid-gestation ultrasound. Ultrasound in Obstetrics & Gynecology. 2012;**40**:140-144. DOI: 10.1002/uog.11175

[41] Simon EG, Arthuis CJ, Haddad G, Bertrand P, Perrotin F. A biparietal/transverse abdominal diameter (BPD/TAD) ratio ≤1: A potential hint for open spina bifida at 11-13 weeks scan. Ultrasound in Obstetrics & Gynecology. Mar 2015;**45**(3):267-272. DOI: 10.1002/uog.13406

[42] Malinger G, Ben-Sira L, Lev D, Ben-Aroya Z, Kidron D, Lerman-Sagie T. Fetal brain imaging: A comparison between magnetic resonance imaging and dedicated neurosonography. Ultrasound in Obstetrics & Gynecology. 2004;**23**(4):333-340

[43] Pugash D, Hendson G, Dunham CP, Dewar K, Money DM, Prayer D. Sonographic assessment of normal and abnormal patterns of fetal cerebral lamination. Ultrasound in Obstetrics & Gynecology. 2012;**40**(6):642-651

[44] Blondiaux E, Sileo C, Nahama-Allouche C, Moutard ML, Gelot A, Jouannic JM, Ducou le Pointe H, Garel C. Periventricular nodular heterotopia on prenatal ultrasound and magnetic resonance imaging. Ultrasound in Obstetrics & Gynecology. 2013;**42**(2):149-155

[45] Howe DT, Rankin J, Draper ES. Schizencephaly prevalence, prenatal diagnosis and clues to etiology: A register-based study. Ultrasound in Obstetrics & Gynecology. 2012;**39**(1):75-82

[46] Tonni G, Pattacini P, Bonasoni MP, Araujo Júnior E. Prenatal diagnosis of lissencephaly type 2 using three-dimensional ultrasound and fetal MRI: Case report and review of the literature. Revista Brasileira de Ginecologia e Obstetrícia. 2016;**38**(4):201-206

[47] Lacalm A, Nadaud B, Massoud M, Putoux A, Gaucherand P, Guibaud L. Prenatal diagnosis of cobblestone lissencephaly associated with Walker-Warburg syndrome based on a specific sonographic pattern. Ultrasound in Obstetrics & Gynecology. 2016;**47**(1):117-122

[48] Guibaud L, Lacalm A. Diagnostic imaging tools to elucidate decreased cephalic biometry and fetal microcephaly: A systematic analysis of the central nervous system. Ultrasound in Obstetrics & Gynecology. 2016;**48**(1):16-25

[49] Leibovitz Z, Daniel-Spiegel E, Malinger G, Tamarkin M, Gindes L, Schreiber L, Ben-Sira L, Lev D, Shapiro I, Bakry H, Weizman B, Zreik A, Egenburg S, Arad A, Tepper R, Kidron D, Lerman-Sagie T. Prediction of microcephaly at birth using three reference ranges for fetal head circumference: Can we improve prenatal diagnosis? Ultrasound in Obstetrics & Gynecology. 2016;**47**(5):586-592

[50] Vinurel N, Van Nieuwenhuyse A, Cagneaux M, Garel C, Quarello E, Brasseur M, Picone O, Ferry M, Gaucherand P, des Portes V, Guibaud L. Distortion of the anterior part of the interhemispheric fissure: Significance and implications for prenatal diagnosis. Ultrasound in Obstetrics & Gynecology. 2014;**43**(3):346-352

[51] Chibueze EC, Parsons AJQ, Lopes KDS, Yo T, Swa T, Nagata C, Horita N, Morisaki N, Balogun OO, Dagvadorj A, Ota E, Mori R, Oladapo OT. Diagnostic accuracy of ultrasound scanning for prenatal microcephaly in the context of Zika virus infection: A systematic review and meta-analysis. Scientific Reports. 2017;**7**(1):2310

[52] Biran-Gol Y, Malinger G, Cohen H, Davidovitch M, Lev D, Lerman-Sagie T, Schweiger A. Developmental outcome of isolated fetal macrocephaly. Ultrasound in Obstetrics & Gynecology. 2010;**36**(2):147-153

[53] Grande M, Arigita M, Borobio V, Jimenez JM, Fernandez S, Borrell A. First-trimester detection of structural abnormalities and the role of aneuploidy markers. Ultrasound in Obstetrics & Gynecology. 2012;**39**(2):157-163

[54] Chaoui R, Heling KS, Thiel G, Karl K. Agnathia-otocephaly with holoprosencephaly on prenatal three-dimensional ultrasound. Ultrasound in Obstetrics & Gynecology. 2011;**37**(6):745-748

[55] Malinger G, Lev D, Kidron D, Heredia F, Hershkovitz R, Lerman-Sagie T. Differential diagnosis in fetuses with absent septum pellucidum. Ultrasound in Obstetrics & Gynecology. 2005;**25**(1):42-49

[56] Blin G, Rabbé A, Mandelbrot L. Prenatal diagnosis of lobar holoprosencephaly using color Doppler: Three cases with the anterior cerebral artery crawling under the skull. Ultrasound in Obstetrics & Gynecology. 2004;**24**(4):476-478

[57] Muresan D, Popa R, Stamatian F, Rotar IC. The use of modern ultrasound tridimensional techniques for the evaluation of fetal cerebral midline structures—A practical approach. Medical Ultrasonography. 2015;**17**(2):235-240

[58] Shen O, Gelot AB, Moutard ML, Jouannic JM, Sela HY, Garel C. Abnormal shape of the cavum septi pellucidi: An indirect sign of partial agenesis of the corpus callosum. Ultrasound in Obstetrics & Gynecology. 2015;**46**(5):595-599

[59] Viñals F, Correa F, Gonçalves-Pereira PM. Anterior and posterior complexes: A step towards improving neurosonographic screening of midline and cortical anomalies. Ultrasound in Obstetrics & Gynecology. 2015;**46**(5):585-594

[60] Cagneaux M, Lacalm A, Huissoud C, Allias F, Ville D, Massardier J, Guibaud L. Agenesis of the corpus callosum with interhemispheric cyst, associated with aberrant cortical sulci and without underlying cortical dysplasia. Ultrasound in Obstetrics & Gynecology. 2013;**42**(5):603-605

[61] Cagneaux M, Guibaud L. From cavum septi pellucidi to anterior complex: How to improve detection of midline cerebral abnormalities. Ultrasound in Obstetrics & Gynecology. 2013;**42**(4):485-486

[62] Paladini D, Pastore G, Cavallaro A, Massaro M, Nappi C. Agenesis of the fetal corpus callosum: Sonographic signs change with advancing gestational age. Ultrasound in Obstetrics & Gynecology. 2013;**42**(6):687-690

[63] Pugash D, Langlois S, Power P, Demos M. Absent cavum with intact septum pellucidum and corpus callosum may indicate midline brain abnormalities. Ultrasound in Obstetrics & Gynecology. 2013;**41**(3):343-344

[64] Santo S, D'Antonio F, Homfray T, Rich P, Pilu G, Bhide A, Thilaganathan B, Papageorghiou AT. Counseling in fetal medicine: Agenesis of the corpus callosum. Ultrasound in Obstetrics & Gynecology. 2012;**40**(5):513-521

[65] Lerman-Sagie T, Ben-Sira L, Achiron R, Schreiber L, Hermann G, Lev D, Kidron D, Malinger G. Thick fetal corpus callosum: An ominous sign? Ultrasound in Obstetrics & Gynecology. 2009;**34**(1):55-61

[66] Shinar S, Har-Toov J, Lerman-Sagie T, Malinger G. Thick corpus callosum in the second trimester can be transient and is of uncertain significance. Ultrasound in Obstetrics & Gynecology. 2016;**48**(4):452-457

[67] Malinger G, Lev D, Oren M, Lerman-Sagie T. Non-visualization of the cavum septi pellucidi is not synonymous with agenesis of the corpus callosum. Ultrasound in Obstetrics & Gynecology. 2012;**40**(2):165-170

[68] Li Y, Estroff JA, Khwaja O, Mehta TS, Poussaint TY, Robson CD, Feldman HA, Ware J, Levine D. Callosal dysgenesis in fetuses with ventriculomegaly: Levels of agreement between imaging modalities and postnatal outcome. Ultrasound in Obstetrics & Gynecology. 2012;**40**(5):522-529

[69] D'Antonio F, Khalil A, Garel C, Pilu G, Rizzo G, Lerman-Sagie T, Bhide A, Thilaganathan B, Manzoli L, Papageorghiou AT. Systematic review and meta-analysis of isolated posterior fossa malformations on prenatal ultrasound imaging (part 1): Nomenclature, diagnostic accuracy and associated anomalies. Ultrasound in Obstetrics & Gynecology. 2016;**47**(6):690-697

[70] D'Antonio F, Khalil A, Garel C, Pilu G, Rizzo G, Lerman-Sagie T, Bhide A, Thilaganathan B, Manzoli L, Papageorghiou AT. Systematic review and meta-analysis of isolated posterior fossa malformations on prenatal imaging (part 2): Neurodevelopmental outcome. Ultrasound in Obstetrics & Gynecology. 2016;**48**(1):28-37

[71] Meagher SE, Walker SP, Choong S. Mid-trimester fetal subdural hemorrhage: Prenatal diagnosis. Ultrasound in Obstetrics & Gynecology. 2002;**20**(3):296-298

[72] Elchalal U, Yagel S, Gomori JM, Porat S, Beni-Adani L, Yanai N, Nadjari M. Fetal intracranial hemorrhage (fetal stroke): Does grade matter? Ultrasound in Obstetrics & Gynecology. 2005;**26**(3):233-243

[73] Vergani P, Strobelt N, Locatelli A, Paterlini G, Tagliabue P, Parravicini E, Ghidini A. Clinical significance of fetal intracranial hemorrhage. American Journal of Obstetrics and Gynecology. 1996;**175**:536-543

[74] Malinger G, Lerman-Sagie T, Watemberg N, Rotmensch S, Lev D, Glezerman M. A normal second-trimester ultrasound does not exclude intracranial structural pathology. Ultrasound in Obstetrics & Gynecology. 2002;**20**:51-56

[75] Ghi T, Simonazzi G, Perolo A, Savelli L, Sandri F, Bernardi B, Santini D, Bovicelli L, Pilu G. Outcome of antenatally diagnosed intracranial hemorrhage: Case series and review of the literature. Ultrasound in Obstetrics & Gynecology. 2003;**22**:121-130

[76] Aziz NA, Peeters-Scholte CM, de Bruine FT, Klumper FJ, Adama van Scheltema PN, Lopriore E, Steggerda SJ. Fetal cerebellar hemorrhage: Three cases with postnatal follow-up. Ultrasound in Obstetrics & Gynecology. 2016;**47**(6):785-786

[77] Garel C, Rosenblatt J, Moutard ML, Heron D, Gelot A, Gonzales M, Miné E, Jouannic JM. Fetal intracerebral hemorrhage and COL4A1 mutation: Promise and uncertainty. Ultrasound in Obstetrics & Gynecology. 2013;**41**(2):228-230

[78] Cruz-Martinez R, Tenorio V, Padilla N, Crispi F, Figueras F, Gratacos E. Risk of ultrasound-detected neonatal brain abnormalities in intrauterine growth-restricted fetuses born between 28 and 34 weeks' gestation: Relationship with gestational age at birth and fetal Doppler parameters. Ultrasound in Obstetrics & Gynecology. 2015;**46**(4):452-459

[79] Buca D, Pagani G, Rizzo G, Familiari A, Flacco ME, Manzoli L, Liberati M, Fanfani F, Scambia G, D'Antonio F. Outcome of monochorionic twin pregnancy with selective intrauterine growth restriction according to umbilical artery Doppler flow pattern of smaller twin: Systematic review and meta-analysis. Ultrasound in Obstetrics & Gynecology. 2017;**50**(5):559-568

[80] Herghelegiu D, Ionescu CA, Pacu I, Bohiltea R, Herghelegiu C, Vladareanu S. Antenatal diagnosis and prognostic factors of aneurysmal malformation of the vein of Galen: A case report and literature review. Medicine (Baltimore). 2017;**96**(30):e7483

[81] Cecchetto G, Milanese L, Giordano R, Viero A, Suma V, Manara R. Looking at the missing brain: Hydranencephaly case series and literature review. Pediatric Neurology. 2013;**48**(2):152-158

[82] Scher MS, Belfar H, Martin J, Painter MJ. Destructive brain lesions of presumed fetal onset: Antepartum causes of cerebral palsy. Pediatrics. 1991;**88**(5):898-906

[83] Pretorius DH, Russ PD, Rumack CM, Manco-Johnson ML. Diagnosis of brain neuropathology in utero. Neuroradiology. 1986;**28**(5-6):386-397

[84] Desvignes F, Beaufrère AM, Biard M, Déchelotte P, Laurichesse-Delmas H, Lemery D, Gallot D. Prenatal diagnosis of cerebral tumors and differential diagnosis. Journal de Gynécologie, Obstétrique et Biologie de la Reproduction. 2013;**42**(3):290-296

[85] Levine D, Jani JC, Castro-Aragon I, Cannie M. How does imaging of congenital Zika compare with imaging of other TORCH infections? Radiology. 2017;**285**(3):744-761

[86] Panigrahy A, Wisnowski JL, Furtado A, Lepore N, Paquette L, Bluml S. Neuroimaging biomarkers of preterm brain injury: Toward developing the preterm connectome. Pediatric Radiology. 2012;**42**(Suppl 1):S33-S61

[87] Madan N, Grant PE. New directions in clinical imaging of cortical dysplasias. Epilepsia. 2009;**50**(Suppl. 9):9-18

[88] Palmini A, Najm I, Avanzini G, Babb T, Guerrini R, Foldvary-Schaefer N, Jackson G, L_ders HO, Prayson R, Spreafico R, Vinters HV. Terminology and classification of the cortical dysplasias. Neurology. 2004;**62**(6 suppl 3):S2-S8